Tetrahedron: *Asymmetry* 20 (2009) 2299–2304

Contents lists available at ScienceDirect

Tetrahedron: *Asymmetry*

journal homepage: www.elsevier.com/locate/tetasy

Enantioselective transesterification catalysis by *Candida antarctica* lipase immobilized on superparamagnetic nanoparticles

Caterina G. C. M. Netto [a], Leandro H. Andrade [b,*], Henrique E. Toma [a,*]

[a] *Supramolecular NanotechLab, Instituto de Quimica, Universidade de São Paulo, São Paulo—SP, Brazil*
[b] *Laboratory of Fine Chemistry and Biocatalysis, Instituto de Quimica, Universidade de São Paulo, São Paulo—SP, Brazil*

ARTICLE INFO

Article history:
Received 4 August 2009
Accepted 20 August 2009
Available online 26 September 2009

ABSTRACT

Lipase B from *Candida antarctica* can be directly immobilized onto functionalized superparamagnetic nanoparticles, preserving its enzymatic activity in the enantioselective transesterification of secondary alcohols, with excellent results in terms of enantiomeric discrimination. The immobilized enzyme can be easily recovered with a magnet, allowing its reuse with negligible loss of activity.

1. Introduction

Green chemistry has intensified the interest toward new catalytic processes, targeting different types of catalysts and enzymes, and improved methods of immobilization.[1] As essential biocatalysts, the enzymes are perfectly adapted to perform with high activity and selectivity under relatively mild conditions. Among the enzymes, lipases are well known for their versatility in organic synthesis, biotechnology, medicinal chemistry, and the food industry. A typical example is lipase B from *Candida Antarctica* (*CALB*), an enzyme capable of performing a wide variety of reactions, such as hydrolysis, transesterification, and aldol reactions.[2] However, one of the problems of using enzymes as catalysts is their serious limitations in terms of recovery;[1h,3] when enhancing the stability and maintaining the activity of the biocatalyst, the choice of the enzyme support is of extreme importance.[4,5]

In this sense, superparamagnetic nanoparticles derived from magnetite (iron oxide) which exhibit a large surface area, and high mass transference, can be easily recovered by using an external magnetic field.[6] In addition to the environmental compatibilities, their use as enzyme support provides an outstanding green chemistry approach, allowing the recovery and extending the useful lifetime of the biocatalyst.

Herein we report a direct procedure for the immobilization of lipase B from *C. antarctica* (CAL-B)[7] onto functionalized magnetic nanoparticles, and a detailed investigation of its catalytic activity in the enantioselective transesterification of substituted secondary alcohols.

2. Results and discussion

The superparamagnetic nanoparticles of magnetite (MagNP) were prepared by the co-precipitation method[6,8] and treated with γ-aminopropyltriethoxysilane (APTS) to yield the APTS-functionalized magnetic nanoparticles, here designated as APTS-MagNP (Scheme 1). The APTS treatment leads to a silicate coating which helps stabilizing the magnetic nanoparticles against oxidation by air. On the other hand, the amino residues are important for preventing the nanoparticle aggregation at pH 7, and for promoting the molecular interactions with the enzyme. The analytical composition of the samples employed in this work was determined as $Fe_3O_4(O_3SiC_3H_8)_{0.29}$, and the transmission electron microscopy revealed the presence of nearly cubic particles, exhibiting a core size distribution from 5 to 10 nm.

Magnetite exhibits a cubic crystallographic cell of 0.83 nm, encompassing eight Fe_3O_4 units.[9] The specific nanoparticle mass can be estimated from the number of crystallographic cells contained in the corresponding nanoparticle volume, as given in Table 1.

Enzyme immobilization was carried out by the addition of CAL-B to the APTS-functionalized magnetic nanoparticles. After work-up, the immobilized lipase nanoparticles, designated as CAL-B/APTS-MagNP were dried under vacuum for 2 h and stored at −7 °C. In addition to the protein analysis based on the Bradford method, the presence of the immobilized enzyme was investigated based on the FTIR spectra of the magnetic nanoparticles, as shown in Figure 1.

The strong peak at 585, 632 cm^{-1} in the magnetic nanoparticles corresponds to the ν(Fe–O) vibrational peak characteristic of bulk magnetite.[10–13] The silica network is adsorbed on the magnetite surface by Fe–O–Si bonds, while the corresponding infrared signals are usually overlapped with the Fe–O band of magnetite. The silane polymer on the surface of the magnetite particles is responsible for the broad vibrational band at 1100–900 cm^{-1}, assigned to the

* Corresponding authors. Tel.: +55 11 3091 3887; fax: +55 11 3815 5579 (H.E.T.).
E-mail addresses: leandroh@iq.usp.br (L.H. Andrade), henetoma@iq.usp.br (H.E. Toma).

0957-4166/$ - see front matter © 2009 Elsevier Ltd. All rights reserved.
doi:10.1016/j.tetasy.2009.08.022

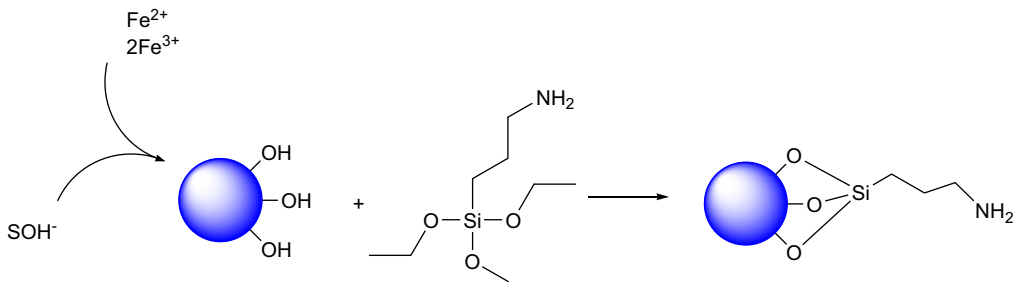

Scheme 1. Synthesis of APTS-functionalized magnetic nanoparticles.

Table 1
Calculated molecular weight (MW) of nanoparticles

Size (nm)	Volume $(nm)^3$	Number of cells	Number of Fe_3O_4 units	MW for Fe_3O_4	MW of $Fe_3O_4(APTS)_{0.29}$
5	125	211	1688	389,928	455,611
6	216	366	2928	676,368	790,303
7	343	5812	4648	1,073,688	1,254,552
8	512	868	6944	1,604,064	1,874,270
9	729	1236	9888	2,284,128	2,668,891
10	1000	1695	13,560	3,132,360	3,660,009

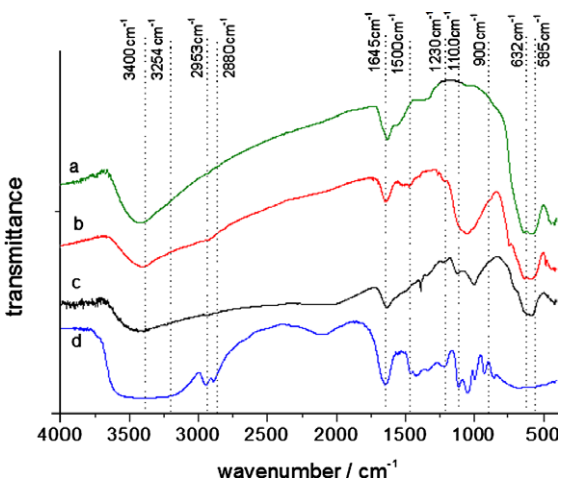

Figure 1. FTIR spectra of (a) MagNP, (b) CAL-B/APTS-MagNP, (c) APTS-MagNP, and (d) CAL-B in KBr pellets.

Si–O–H and Si–O–Si groups. The weak bands at 3417 and 1625 cm^{-1} are ascribed to the N–H stretching and H–N–H bending modes of the free/protonated amino group, respectively.[14,15] Hydrogen-bonded silanols also absorb at around 3200 and 3470 cm^{-1}.[14,16]

The FTIR spectrum of CAL-B (Fig. 1d) shows the characteristic amide I[17] band at 1645 cm^{-1} , while the amide II band appears around 1500 cm^{-1}. The amide III and IV bands are observed at 1328 cm^{-1} and 610 cm^{-1}. The vibrational peaks around 1100–1000 cm^{-1} are associated with the C–C and C–N composite vibrations of the protein chain.

When CAL-B is immobilized onto APTS-MagNP (Fig. 1b) there is a strong overlap of the vibrational peaks of the enzyme (amide I) and nanoparticles at 1645 cm^{-1} (amide I), but the characteristic amide I band is observed at 1500 cm^{-1}. In addition, there is a strong enhancement of the vibrational peaks in the 1500–900 cm^{-1} region, involving the amide III, and the skeletal C–C, C–N, and Si–O vibrations. Although a detailed assignment is not possible at the present time because of the complexity involved, the observed changes in the vibrational spectra corroborate the binding of the CAL-B enzyme to APTS-MagNP.

The binding of CAL-B lipase to APTS-MagNP was found to be strong enough to resist successive washing processes, yielding reproducible results. Presumably, the binding of the enzyme to APTS-MagNP is driven by hydrogen bonding and electrostatic interactions, since at pH 7, CAL-B has a negative charge (isoelectric point = 6)[18] and the magnetic nanoparticles exhibit a positive charge due to the protonation of the aliphatic amines ($pK_a \sim 9$).[19] In addition, there are many amide and aminoacid residues in CAL-B available for interacting with the protonated amine groups of APTS-MagNP.

Before the catalytic tests, the enzyme immobilization procedure was optimized by varying the temperature, concentration, immobilization time, and washing procedures. The amount of adsorbed protein was determined by monitoring the total and the remaining concentrations of the enzyme in the solution, using the Bradford method.[20]

For the purpose of discussion, the immobilization of the CAL-B enzyme on the magnetic nanoparticles (APTS-MagNP) can be represented by

$$n\text{CAL-B} + \text{APTS-MagNP} \rightleftharpoons \text{APTS-MagNP(CAL-B)}_n$$

where

$$K = \frac{[\text{APTS-MagNP(CAL-B)}_n]}{[\text{CAL-B}]^n[\text{APTS-MagNP}]} \quad (1)$$

The kinetics involved were evaluated from the amount of the absorbed protein as a function of time, as shown in Figure 2.

As can be seen in Figure 2, the binding process requires about 4 h for equilibration. This observation indicates that specific interactions between the enzyme and the APTS-coated nanoparticles should take place, rather than just a diffusion-controlled physical adsorption process.

The extent of immobilization also depends on the amounts of MagNP employed in the experiments. For a constant mass of enzyme, there is a non-linear increase of the immobilized enzyme versus the amount of MagNP, as shown in Figure 3.

Based on the data shown in Figure 3 and Table 1, one can evaluate the equilibrium constants for the interaction of CAL-B and APTS-MagNP by inserting the known concentrations of the enzyme ($[\text{CAL-B}]_{total}$), and of the immobilized species, [APTS-MagNP(CAL-B)$_n$] into the corresponding equations.

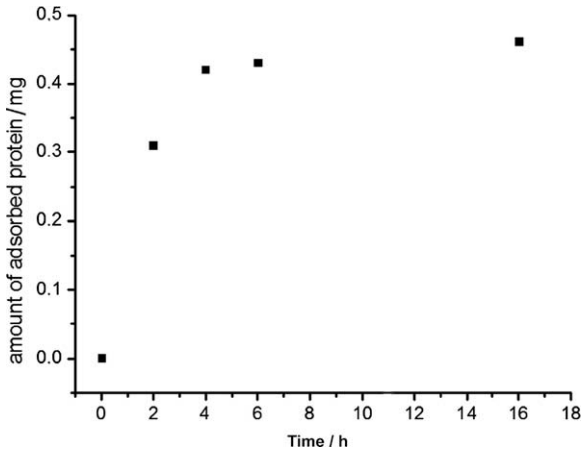

Figure 2. Kinetics of immobilization of CAL-B (5.2 mg/mL) on APTS-MagNP (30 mg/mL) at 32 °C.

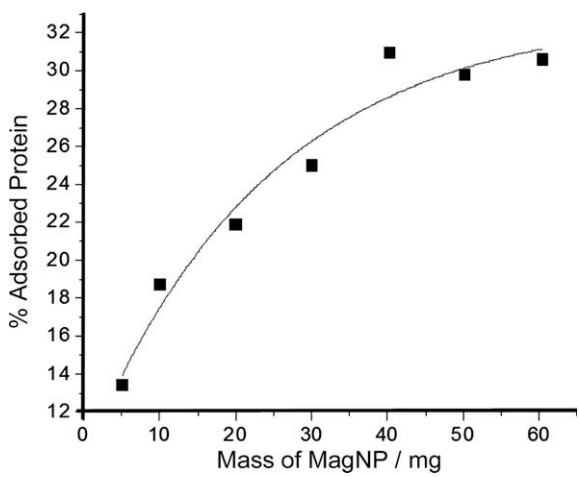

Figure 3. Relative amounts of adsorbed protein *vs* the mass of APTS-MagNP used in the immobilization process.

Considering that

$$[\text{APTS-MagNP(CAL-B)}_n] = nx$$

$$[\text{CAL-B}]_{\text{free}} = [\text{CAL-B}]_{\text{total}} - nx$$

$$[\text{APTS-MagNP}]_{\text{free}} = [\text{APTS-MagNP}]_{\text{total}} - x$$

Equations can be expressed in the following ways, for

$$n = 1 \quad K = x/\{[\text{CAL-B}]_{\text{total}} - x\}\{[\text{APTS-MagNP}]_{\text{total}} - x\} \tag{2}$$

$$n = 2 \quad K = 2x/\{[\text{CAL-B}]_{\text{total}} - 2x\}^2\{[\text{APTS-MagNP}]_{\text{total}} - x\} \tag{3}$$

$$n = 3 \quad K = 3x/\{[\text{CAL-B}]_{\text{total}} - 3x\}^3\{[\text{APTS-MagNP}]_{\text{total}} - x\} \tag{4}$$

Although the values of x are experimentally known, the concentration of the magnetic nanoparticles $[\text{APTS-MagNP}]_{\text{total}}$ depends upon the molecular weight assumed for the different sizes (Table 1), and this point should be taken into consideration in the calculations. For $n = 1$ and 2, the calculated values of K were typically negative and can be discarded for the majority of the concentrations of the APTS-MagNP employed, assuming a nanoparticle size distribution from 5 to 10 nm. However, in the case of $n = 3$, the calculated values of K were positive and constant within one order of magnitude, as one can see in Table 2. The average constant ($K_{1:3}$) was 1.41×10^{13} mol^{-3} dm^9 at 32 °C.

The influence of the temperature on the immobilization yield was also investigated. As shown in Figure 4, when the temperature increases, the amount of adsorbed enzymes decreases. The calculation of the association constants at 37 and 42 °C led to $K_{1:3} = 2.96 \times 10^{12}$ and 8.53×10^{11} mol^{-3} dm^9, respectively. The corresponding thermodynamic parameters based on the Gibbs equation were obtained from the linear plot of ln K versus $1/T$ (Fig. 4 inset) as $\Delta H = -220$ kJ mol^{-1} and $\Delta S = -480$ J mol^{-1} K^{-1}. It should be mentioned that CAL-B undergoes 50% denaturation only at 53 °C,[21] quite far from the temperatures employed in the immobilization procedure. Therefore, the thermodynamic data are consistent with relatively strong chemical interactions, presumably involving hydrogen bonds between CAL-B and the magnetic nanoparticles, rather than a simple adsorption process.

After carrying out a controlled and reproducible binding of CAL-B on the APTS-modified magnetic nanoparticles, a systematic study was performed to evaluate their enantioselective behavior on the transesterification reaction of secondary alcohols. In particular,

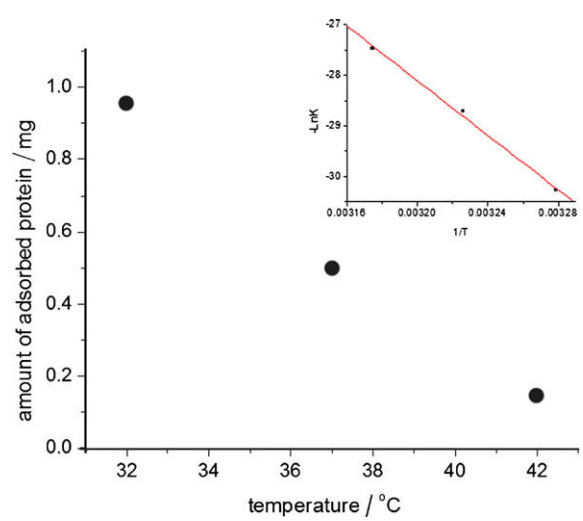

Figure 4. Effect of temperature on the enzyme binding to the magnetic nanoparticles (30 mg) showing the linear ln K versus $1/T$ plot in the inset.

Table 2
Calculated association constants, $K_{1:3}$ (mol^{-3} dm^9) based on Eq. 4, assuming the [MagNP(CAL-B)$_3$] composition (32 °C), for several amounts of MagNP and different nanoparticles size

Size (nm)	Mass (mg)						
	5	10	20	30	40	50	60
5	2.03×10^{13}	9.85×10^{12}	2.53×10^{12}	4.47×10^{12}	4.68×10^{12}	3.51×10^{12}	3.12×10^{12}
6		2.39×10^{13}	5.10×10^{12}	8.63×10^{12}	8.12×10^{12}	6.55×10^{12}	5.75×10^{12}
7		8.52×10^{13}	1.04×10^{13}	1.63×10^{13}	1.29×10^{13}	1.16×10^{13}	9.99×10^{12}
8			2.52×10^{13}	3.26×10^{13}	1.92×10^{13}	2.04×10^{13}	1.71×10^{13}
9			1.73×10^{14}	8.17×10^{13}	2.74×10^{13}	3.77×10^{13}	2.98×10^{13}
10				2.28×10^{15}	3.76×10^{13}	8.23×10^{13}	5.69×10^{13}

the enantioselective acetylation of alcohols derived from (*R,S*)-1-phenylethanol mediated by CAL-B/APTS-MagNP was investigated.

In order to demonstrate the characteristic catalytic activity for lipases, we first examined the performance of the CAL-B/APTS-MagNP in the hydrolysis of *para*-nitrophenyl palmitate. In this case, the observed activity was about 0.8 U/mg for immobilized CAL-B, while that for free CAL-B was 0.4 U/mg. The activity of CAL-B increased by a factor of 2 in the immobilized form.

The enantioselective activity of CAL-B/APTS-MagNP was then evaluated in the transesterification reactions using (*RS*)-1-phenyl-ethanol (*para*-nitro, *para*-methyl, *para*-bromo, *para*-chloro, and *para*-methoxy derivatives) in the presence of vinyl acetate as an acyl donor. All the reactions exclusively yielded the corresponding (*R*)-1-phenylethyl acetate, as shown in Figure 5, demonstrating the successful use of CAL-B/APTS/MagNP as catalyst in the kinetic resolution of secondary alcohols via transesterification reaction.

As a matter of fact, it is known that the CAL-B enzyme is highly selective for the (*R*)-enantiomer of the secondary alcohols because there is a physical restriction in the active site, generating a stereospecific pocket to accommodate the methyl group of 1-phenylethanol, in the (*R*)-configuration.[22]

Table 3 summarizes the results obtained for all the reactions tested. It is noteworthy that the (*R*)-enantiomer from the racemic mixture of substituted 1-phenylethanols **1a–f** was acetylated with excellent enantioselectivity, >99%. The enantiomeric ratio *E* (*E-value*), given by Eq. 5,[1] was quite high (*E* >300) for all the reactions investigated (Table 1) reflecting the high specificity of the CAL-B immobilized on the superparamagnetic nanoparticles.

$$E = \ln\{(1 - ee_s)/(1 + ee_s/ee_p)\}/\ln\{(1 + ee_s)/(1 + ee_s/ee_p)\} \quad (5)$$

where ee_p refers to the enantiomeric excess of the product and ee_s refers to the enantiomeric excess of the substrate.

In order to evaluate the recycling potential of the CAL-B immobilized on the supermagnetic nanoparticles, a series of repetitive experiments were carried out for the transesterification reaction using (*R,S*)-1-phenylethanol **1a** as a substrate. After each process, the catalytic particles were collected with a magnet, washed, and used again in a new experiment. As shown in Figure 6, the immobilized enzyme maintained its activity, exhibiting less than 5% decay after four cycles. The *E-value* and the enantiomeric excess of product **2a** were the same after each cycle, that is, >300% and >99%, respectively).

3. Conclusion

The adsorption of lipase B from *C. antarctica on* magnetic nanoparticles provides an efficient strategy in enzymatic catalysis, preserving its highly enantioselective activity in the transesterification of secondary alcohols. More important, the immobilized enzyme can be conveniently recovered with a magnet and used at least four times, with negligible loss of activity.

4. Experimental

4.1. Materials

All commercially available chemicals were used without further purification. Ferric chloride hexahydrate ($FeCl_3{\cdot}6H_2O$, >98%) and ferrous chloride ($FeCl_2$, 98%) were obtained from Sigma–Aldrich. Toluene (99.9%), monobasic sodium phosphate monohydrate ($NaH_2PO_4{\cdot}H_2O$, >99%), and dibasic sodium phosphate (HNa_2PO_4, 99%) were obtained from Merck. Sodium hydroxide (NaOH, 97%), ethanol (99.8%), and methanol (99.9%) were obtained from Synth. γ-Aminopropyltriethoxisilane was obtained from Pierce. *C. antarctica* Lipase B (CALB-L) was donated by Novozymes (Parana-Brazil). Phenylethanols (*RS*)-**1a–f** were prepared by reduction of the corresponding commercially available acetophenones (Sigma–Aldrich) with $NaBH_4$ in methanol. The acetates (*RS*)-**2a–f** were prepared by acetylation of the precursor alcohols (*RS*)-**1a–f** by reacting with acetic anhydride in dichloromethane, triethylamine, and 4-(*N,N*-dimethylamino)pyridine as catalyst.

4.2. Synthesis of superparamagnetic nanoparticles

Superparamagnetic nanoparticles of magnetite were obtained by the co-precipitation method. A solution of Fe^{2+} and Fe^{3+} ions (0.1 mol/L and 0.2 mol/L, respectively) was slowly dropped into a solution of NaOH (0.5 mol/L). To protect the nanoparticles against oxidation a flow of N_2 was maintained during the reaction. The reaction mixture was kept under mechanical stirring (2000 rpm) for 30 min. After this period, the black suspension obtained was washed several times with deoxygenated Milli-Q water until pH 7 was reached.

4.3. Nanoparticles surface modification

For the surface modification of the nanoparticles, an adaptation of the Kim et al. method was used.[22] After confining the particles with the help of an external magnetic field, the black solid was washed three times with 50 mL of analytical grade methanol. This material was dispersed in 70 mL of toluene/methanol mixture (1:1) and heated at 95 °C under N_2 atmosphere until 50% of the solution volume was evaporated. After the evaporation, 35 mL of methanol was added and the mixture was re-evaporated to one-half. This procedure was repeated until the residual water was

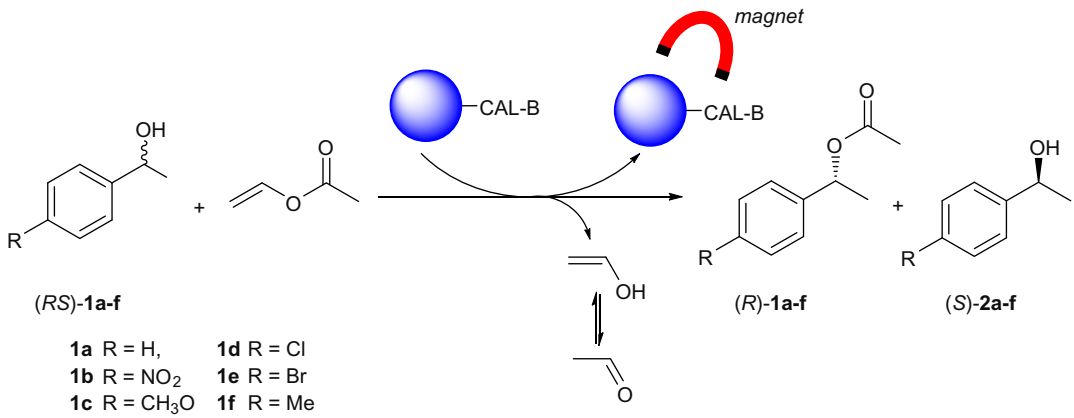

Figure 5. Application of CAL-B/APTS/MagNP as a catalyst in the kinetic resolution of secondary alcohols via a transesterification reaction.

Table 3
Kinetic resolution of (*RS*)-1-phenylethanols **1a**–**f** via transesterification reaction catalyzed by CAL-B supported on supermagnetic nanoparticles[a]

Substrate	Vinyl acetate (mmol)	Time (h)	(*S*)-**1a**–**f** ee[c] (%)	(*R*)-**2a**–**f** ee[c] (%)	Conv.[d] (%)	*E*[e]
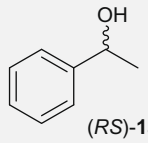 (*RS*)-**1a**	5	6	13	>99	12	226
		24	48	>99	32	320
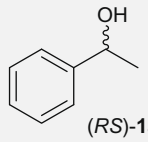 (*RS*)-**1a**	50[b]	24	76	>99	43	458
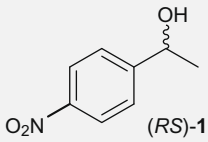 (*RS*)-**1b**	5	6	13	>99	12	226
		24	48	>99	32	320
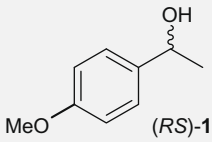 (*RS*)-**1c**	5	6	19	>99	16	239
		24	55	>99	36	346
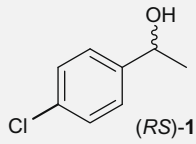 (*RS*)-**1d**	5	6	21	>99	17	264
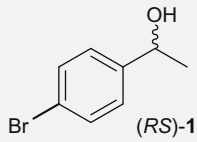 (*RS*)-**1e**	5	6	32	>99	25	319
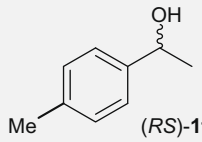 (*RS*)-**1f**	5	6	35	>99	26	320

[a] Reaction conditions: substrate (1 mmol) **1a**–**f**, methyl *tert*-butyl ether (1 mL); 32 °C, 30 mg of CAL-B/APTS-MagNP (this system contains 0.4 mg of the CAL-B).
[b] 10 mmol of (*RS*)-1-phenylethanol and 300 mg of CAL-B/APTS-MagNP (This system contains 4 mg of the CAL-B).
[c] ee = Enantiomeric excess was determined by chiral GC analysis.
[d] Conv. = Conversion = $ee_s/ee_s + ee_p$.
[e] $E = \ln\{(1 - ee_s)/(1 + ee_s/ee_p)\}/\ln\{(1 + ee_s)/(1 + ee_s/ee_p)\}$.

thoroughly removed. Then, the γ-aminopropyltriethoxysilane (0.2 mL/mg of the magnetic nanoparticle) was added to the magnetic nanoparticles. The suspension was heated under N_2 and refluxed at 110 °C through 12 h. After the surface modification the suspension was confined using a magnet, and the solid was washed 10 times with 10 mL of methanol and 10 mL of ethanol, and then dried under vacuum for 24 h. Elementary Anal. Calcd for $Fe_3O_4(O_3SiC_3H_8N)_{0.29}$: C, 3.4; H, 0.76; N, 1.32. Found: C, 3.8; H, 0.83; N, 1.11.

4.4. CAL-B immobilization

Magnetic nanoparticles (30 mg) were dispersed in 1 mL of phosphate buffer solution (pH 7.0, 0.1 M). Then, 600 μL of lipase B from *C. antarctica* (5.2 mg/mL, protein content) was added into the suspension and the resulting mixture was stirred on an orbital shaker at 32 °C and 160 rpm for 2 h. After the immobilization time, the magnetic nanoparticles were washed three times with phosphate buffer solution (pH 7, 3 × 0.5 mL), dried at vacuum for 2 h, and then stored at −7 °C.

The Bradford method[20] was used for determining the amount of the protein in the supernatant using Bovine Serum Albumin as standard. By carrying out a mass balance, the amount of lipase immobilized into the magnetic nanoparticles was evaluated. A visible-UV HP 8453-A spectrophotometer from Hewlett Packard was employed for the determination of the protein content.

4.5. Nanoparticle characterization

The characterization of the magnetic nanoparticles was carried out as previously reported.[8] Relevant vibrational information confirming the presence of the enzyme in the CAL-B/APTS-MagNPs

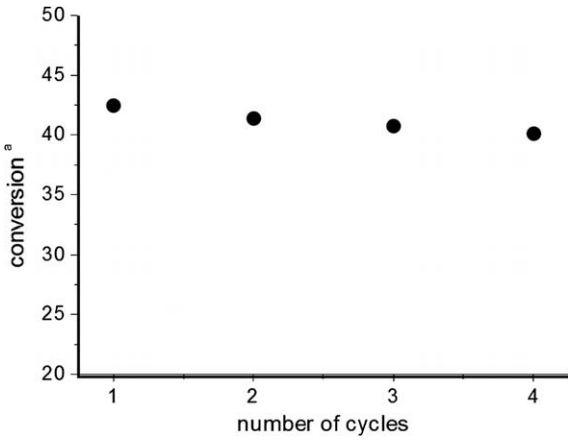

Figure 6. Recycling behavior of CAL-B immobilized on magnetite nanoparticles for kinetic resolution of the (*RS*)-1-phenylethanol *rac*-**1a**: 30 mg of CAL-B/APTS-MagNP; 1 mmol of *rac*-**1a**; 5 mmol of vinyl acetate; 6 h at 32 °C; [a]conversion expressed as $c = ee_s/ee_s + ee_p$.

was obtained with Fourier transform infrared spectroscopy (FTIR-8300, SHIMADZU) using KBr pellets. Each spectrum was collected after accumulating 50 scans at a resolution of 2 cm^{-1}.

4.6. General procedure for the kinetic resolution of the alcohols (*RS*)-1a–f

To a 10 mL glass flask containing 1 mL of MTBE (methyl-*tert*-butyl ether), 50 μL of vinyl acetate (5 mmol), and 30 mg immobilized enzyme on magnetic nanoparticles (0.4 mg protein/30 mg magnetic nanoparticle) was added the appropriate alcohol **1a–f** (1 mmol). The reaction mixture was stirred on a rotary shaker (32 °C, 160 rpm) for the appropriate time (Table 1). After this, the mixture was filtered and the solvent was evaporated.

4.7. Evaluation of the enzymatic kinetic resolutions

After the reaction time given in Table 1, the samples were analyzed by GC analysis using a chiral capillary column. The enantiomeric excess of the compounds were determined by chromatographic comparison with authentic samples of (*RS*)-alcohols **1a-e** and (*RS*)-acetates **2a–e** synthesized chemically (see Section 4.1).

GC conditions (carrier gas-H_2, 100 kPa): injector 220 °C, detector 220 °C, column temperature, and retention time, t_R (min), for each compound are indicated below.

(*RS*)-phenylethanol **1a**: Isotherm at 107 °C, (*R*)-enantiomer 6.22 min, and (*S*)-enantiomer 6.87 min.

(*RS*)-1-(4-Nitrophenyl)ethanol **1b**: Isotherm at 150 °C, (*R*)-enantiomer 19.92 min, and (*S*)-enantiomer 20.30 min.

(*RS*)-1-(4-Methoxyphenyl)ethanol **1c**: Isotherm at 119 °C, (*R*)-enantiomer 6.22 min, and (*S*)-enantiomer 6.87 min.

(*RS*)-1-(4-Bromophenyl)ethanol **1d**: Isotherm at 135 °C, (*R*)-enantiomer 9.54 min, and (*S*)-enantiomer 10.52 min.

(*RS*)-1-(4-Chlorophenyl)ethanol **1e** Isotherm at 130 °C, (*R*)-enantiomer 7.33 min, and (*S*)-enantiomer 8.19 min.

(*RS*)-1-(4-Methylphenyl)ethanol **1f**: Isotherm at 113 °C, (*R*)-enantiomer 6.79 min, and (*S*)-enantiomer 7.71 min.

(*RS*)-1-Phenylethyl acetate **2a**: 110 °C up to 103 °C, 1 °C/min, (*R*)-enantiomer 4.35 min, and (*S*)-enantiomer 5.05 min.

(*RS*)-1-(4-Nitrophenyl)ethyl acetate **2b**: Isotherm at 150 °C, (*R*)-enantiomer 9.44 min, and (*S*)-enantiomer 10.23 min.

(*RS*)-1-(4-Methoxyphenyl)ethyl acetate **2c**: Isotherm at 110 °C, (*R*)-enantiomer 11.79 min, and (*S*)-enantiomer 13.47 min.

(*RS*)-1-(4-Bromophenyl)ethyl acetate **2d**: Isotherm at 135 °C, (*R*)-enantiomer 6.93 min, and (*S*)-enantiomer 7.75 min.

(*RS*)-1-(4-Chlorophenyl)ethyl acetate **2e**: Isotherm at 130 °C, (*R*)-enantiomer 5.31 min, and (*S*)-enantiomer 6.00 min.

(*RS*)-1-(4-Methylphenyl)ethyl acetate **2f**: 93 °C up to 113 °C, 1 °C/min, (*R*)-enantiomer 10.43 min, and (*S*)-enantiomer 11.75 min.

4.8. Absolute configuration

The absolute configurations of all compounds were determined by comparison of the sign of the measured specific rotation with those in the literature.[1]

4.9. Enzymatic activity assay using the hydrolysis of *para*-nitrophenyl palmitate (*p*NPP)

The activity assay was done by monitoring at 410 nm the appearance of *para*-nitrophenol during the hydrolysis of *p*NPP as substrate, in accordance with the procedure reported by Teng et al.[23] One unit of lipase activity is defined as the amount of lipase which catalyzed the production of 1 μmol of the *para*-nitrophenol per minute under the experimental conditions.

Acknowledgments

The authors acknowledge the support from FAPESP, CNPq, and PETROBRAS, and Professor Pedro K. Kyohara (Institute of Physics, Univ. S. Paulo) for obtaining TEM images of APTS-MagNP.

References

1. (a) Chakraborty, S.; Sahoo, B.; Teraoka, I.; Miller, L. M.; Gross, R. A. *Macromolecules* **2005**, *38*, 61; (b) Huang, S.-H.; Liao, M.-H.; Chen, D.-H. *Biotechnol. Prog.* **2003**, *19*, 1095; (c) Torres, R.; Ortiz, C.; Pessela, B. C. C.; Palomo, J. M.; Mateo, C.; Guisan, J. M.; Fernandez-Lafuente, R. *Enzyme Microb. Technol.* **2006**, *39*, 167; (d) Reetz, M. T.; Zonta, A.; Vijayakrishnan, V.; Schimossek, K. *J. Mol. Catal. A: Chem.* **1998**, *134*, 251; (e) Hung, T.-C.; Giridhar, R.; Chiou, S.-H.; Wu, W.-T. *J. Mol. Catal. B: Enzym.* **2003**, *26*, 69; (f) Guo, Z.; Sun, Y. *Biotechnol. Prog.* **2004**, *20*, 500; (g) Fernandez-Lorente, G.; Palomo, J. M.; Mateo, C.; Munilla, R.; Ortiz, C.; Cabrera, Z.; Guisan, J. M.; Fernandez-Lafuente, R. *Biomacromolecules* **2006**, *7*, 2610; (h) Mateo, C.; Palomo, J. M.; Fernandez-Lorente, G.; Guisan, J. M.; Fernandez-Lafuente, R. *Enzyme Microb. Technol.* **2007**, *40*, 1451; (i) Dallavecchia, R.; Sebrão, D.; Nascimento, M. G.; Soldi, V. *Process Biochem.* **2005**, *40*, 2677–2682; (j) Nascimento, M. G.; Queiroz, N. *Tetrahedron Lett.* **2002**, *43*, 5225–5227.
2. (a) Fujii, R.; Nakagawa, Y.; Hiratake, J.; Sogabe, A.; Sakata, K. *Protein Eng. Des. Sel.* **2005**, *18*, 93; (b) Torres-Gavilan, A.; Castillo, E.; Lopez-Munguıa, A. *J. Mol. Catal. B: Enzym.* **2006**, *41*, 136; (c) Branneby, C.; Carlqvist, P.; Hult, K.; Brinck, T.; Berglund, P. *J. Mol. Catal. B: Enzym.* **2004**, *31*, 123; (d) Carlqvist, P.; Magnusson, A.; Hult, K.; Brinck, T.; Berglund, P. *J. Am. Chem. Soc.* **2003**, *125*, 874; (e) Svedendahl, M.; Hult, K.; Berglund, P. *J. Am. Chem. Soc.* **2005**, *127*, 17988; (f) Hong-Xia, D.; Shi-Ping, Y.; Jian, W. *Biotechnol. Lett.* **2006**, *28*, 1503; (g) Torre, O.; Alfonso, I.; Gotor, V. *Chem. Commun.* **2004**, 1724.
3. Herdt, A. R.; Kim, B.-S.; Taton, T. A. *Bioconjugate Chem.* **2007**, *18*, 183.
4. Sabbani, S.; Hendentröm, E.; Nordin, O. *J. Mol. Catal. B: Enzym.* **2006**, *42*, 1–9.
5. Willner, I.; Katz, E. *Langmuir* **2006**, *22*, 1409–1419.
6. Kim, D. K.; Mikhaylova, M.; Zhang, Y.; Muhammed, M. *Chem. Mater.* **2003**, *15*, 1617–1627.
7. Kirk, O.; Christensen, W. *Org. Process Res.* **2002**, *6*, 446.
8. Yamaura, M.; Camilo, R. L.; Sampaio, L. C.; Macedo, M. A.; Nakamura, M.; Toma, H. E. *J. Magn. Magn. Mater.* **2004**, *279*, 210–217.
9. Cornell, R. M.; Schwertmann, U. *The Iron Oxides*; Wiley: Weinheim, 2003.
10. Waldron, R. D. *Phys. Rev.* **1955**, *99*, 1727.
11. Ma, M.; Zhang, Y.; Yu, W.; Shen, H.-Y.; Zhang, H.-Q.; Gu, N. *Colloids Surf., A* **2003**, *212*, 219.
12. Guang-She, L.; Li-Ping, L.; Smith, R. L., Jr.; Inomata, H. *J. Mol. Struct.* **2001**, *560*, 87.
13. Bruni, S.; Cariati, F.; Casu, M.; Lai, A.; Misunu, A.; Piccaluga, G.; Solinas, S. *Nanostruct. Mater.* **1999**, *11*, 573.
14. White, L. D.; Tripp, C. P. *J. Colloid Interface Sci.* **2000**, *232*, 400.
15. Xu, Z.; Liu, Q.; Finch, J. A. *Appl. Surf. Sci.* **1997**, *120*, 269.
16. Ramesh, S.; Felner, I.; Koltypin, Y.; Gedanken, A. *J. Mater. Res.* **2000**, *15*, 944.
17. Stuart, B. *Infrared Spectroscopy: Fundamentals and Applications*; Oxford, 2004.
18. Christensen, M. W.; Kirk, O. *Org. Process Res. Dev.* **2002**, *6*, 446.
19. *Handbook of Chemistry and Physics*, 67ª ed.; CRC Press: Florida, USA.
20. Bradford, M. M. *Anal. Biochem.* **1976**, *72*, 248.
21. Bovet, C.; Zenobi, R. *Anal. Biochem.* **2008**, *373*, 380.
22. Uppenberg, J.; Öhmer, N.; Norin, M.; Hult, K.; Kleywegt, G. J.; Patkar, S.; Waagen, V.; Anthonsen, T.; Jones, T. A. *Biochemistry* **1995**, *34*, 16838–16851.
23. Teng, Y.; Xu, Y. *Anal. Biochem.* **2007**, *363*, 297.